


Lipocalin 2 expression promotes tumor progression and therapy resistance by inhibiting ferroptosis in colorectal cancer

Nazia Chaudhary^{1,2} | Bhagya Shree Choudhary^{1,2} | Sanket Girish Shah^{2,3} |
Nileema Khapare¹ | Nehanjali Dwivedi⁴ | Anagha Gaikwad¹ | Neha Joshi¹ |
Jinsy Raichanna¹ | Srikanta Basu¹ | Murari Gurjar⁵ | Smitha P.K.⁴ |
Avanish Saklani⁶ | Poonam Gera⁷ | Mukta Ramadwar⁸ | Prachi Patil⁹ |
Rahul Thorat¹⁰ | Vikram Gota^{5,2} | Sujan K. Dhar¹¹ | Sanjay Gupta^{3,2} |
Manjula Das^{4,11} | Sorab N. Dalal^{1,2} 

¹Cell and Tumor Biology, Advanced Centre for Treatment, Research and Education in Cancer (ACTREC), Tata Memorial Centre, Navi Mumbai, India

²Life Sciences, Homi Bhabha National Institute, Mumbai, India

³Epigenetics and Chromatin Biology Group, Gupta Lab, Advanced Centre for Treatment, Research and Education in Cancer (ACTREC), Tata Memorial Centre, Navi Mumbai, India

⁴Tumor Immunology Program, Mazumdar Shaw Medical Foundation, Mazumdar Shaw Medical Centre, Narayana Health City, Bangalore, India

⁵Department of Clinical Pharmacology, Advanced Centre for Treatment, Research and Education in Cancer (ACTREC), Tata Memorial Centre, Navi Mumbai, India

⁶Department of Gastrointestinal Oncology, Tata Memorial Hospital, Tata Memorial Centre, Mumbai, India

⁷Department of Biorepository, Advanced Centre for Treatment, Research and Education in Cancer (ACTREC), Tata Memorial Centre, Navi Mumbai, India

⁸Department of Pathology, Tata Memorial Hospital, Tata Memorial Centre, Mumbai, India

⁹Department of Digestive Disease and Clinical Nutrition, Tata Memorial Hospital, Tata Memorial Centre, Mumbai, India

¹⁰Laboratory Animal Facility, Advanced Centre for Treatment, Research and Education in Cancer (ACTREC), Tata Memorial Centre, Navi Mumbai, India

Abstract

Lipocalin 2 is a siderophore-binding protein that regulates iron homeostasis. Lipocalin 2 expression is elevated in multiple tumor types; however, the mechanisms that drive tumor progression upon Lipocalin 2 expression remain unclear. When Lipocalin 2 is over-expressed, it leads to resistance to 5-fluorouracil in colon cancer cell lines in vitro and in vivo by inhibiting ferroptosis. Lipocalin 2 inhibits ferroptosis by decreasing intracellular iron levels and stimulating the expression of glutathione peroxidase4 and a component of the cysteine glutamate antiporter, xCT. The increase in xCT levels is dependent on increased levels of ETS1 in Lipocalin 2 over-expressing cells. Inhibiting Lipocalin 2 function with a monoclonal antibody leads to a decrease in chemo-resistance and transformation in vitro, and a decrease in tumor progression and chemo-resistance in xenograft mouse models. Lipocalin 2 and xCT levels exhibit a positive correlation in human tumor samples suggesting that the pathway we have identified in cell lines is operative in human tumor samples. These results indicate that Lipocalin 2 is a potential therapeutic target and that the monoclonal antibody described in our study can serve as the basis for a potential therapeutic in patients who do not respond to chemotherapy.

KEYWORDS

chemo-resistance, colorectal cancer, ferroptosis, Lipocalin 2

What's new?

Lipocalin 2 (LCN2) regulates iron homeostasis, and is elevated in many tumor types. In this study, the authors found that increased LCN2 levels were correlated with increased resistance to 5-fluorouracil. This resistance was due to the ability of LCN2 to inhibit ferroptosis, an iron-dependent cell-death mechanism. However, blocking LCN2 function with a monoclonal

Abbreviations: 5FU, 5-fluorouracil; ACTREC, Advanced Centre for Treatment Research and Education in Cancer; DFO, deferoxamine; FER, ferrostatin; ETS1, ETS Proto-Oncogene 1; GPX4, glutathione peroxidase4; GSH, glutathione; IEC III, Institute Ethics Committee III; IAEC, Institute Animal Ethics Committee; LCN2, Lipocalin 2; LIP, liproxstatin; MMP9, matrix-metalloprotease-9; mIgG, mouse immunoglobulin G; NAC, N-acetyl cysteine; NACTRT, neoadjuvant chemoradiotherapy; NEC, necrostatin; PKP3, plakophilin3; qRT-PCR, quantitative reverse transcriptase coupled PCR; ROS, reactive oxygen species; TMC, Tata Memorial Centre; TMH, Tata Memorial Hospital.

¹¹Beyond Antibody, InCyte Laboratory, Mazumdar Shaw Medical Foundation, Mazumdar Shaw Medical Centre, Narayana Health City, Bangalore, India

Correspondence

Sorab N. Dalal, Advanced Centre for Treatment, Research and Education in Cancer (ACTREC), Tata Memorial Centre, Kharghar, Navi Mumbai 410210, India.
Email: sdalal@actrec.gov.in

Funding information

ACTREC donation fund, Grant/Award Number: 4338; Department of Biotechnology, Government of India, Grant/Award Number: BT/PR8351/MED/30/995/2013

antibody sensitized cells to therapy and inhibited tumor growth in vivo. These results indicate that Lipocalin 2 is a potential therapeutic target, and that similar antibodies may offer a new therapeutic strategy for tumors with high LCN2 levels.

1 | INTRODUCTION

The first line of treatment in patients with colorectal cancer (CRC) is curative surgery.¹ Post-surgery, adjuvant chemotherapy comprising 5-fluorouracil (5FU) and Oxaliplatin is given to patients with Stages III and IV colon cancer.¹ The standard of care for patients with locally advanced rectal cancer is neoadjuvant chemoradiotherapy (NACTRT), 45–50 Gy of radiation over 5–6 wk and Capecitabine (an orally administered prodrug of 5FU) at a dose of 825 mg/m² twice daily. Responders to NACTRT with tumors that are deemed operable undergo surgery, while the non-responders undergo further rounds of chemotherapy followed by surgery if the disease becomes operable.² A large number of patients relapse and develop drug-resistant disease.¹ Multiple mechanisms might contribute to therapy resistance in CRC³; however, markers that predict therapy response or targeted therapies that can overcome therapy resistance are not available in the clinic.

Ferroptosis is an iron-dependent cell death mechanism distinct from other forms of cell death, such as apoptosis and necroptosis.⁴ The induction of ferroptosis is dependent on the presence of reactive iron radicals⁵ and an inability to reduce peroxidated phospholipids. The failure to reduce peroxidated phospholipids is due to either a decrease in the enzyme glutathione peroxidase4 (GPX4)^{6,7} or due to a reduction in glutathione (GSH) production due to a reduction in Cysteine import by system x_c[−].⁸ Consistent with these observations, compounds that inhibit the accumulation of lipid peroxides such as liproxstatin (LIP)⁹ and ferrostatin (FER)⁵ inhibit ferroptosis, while compounds that inhibit the activity of GPX4 (RSL3) or the system x_c[−] component, xCT (Erastin),^{10–12} promote ferroptotic cell death. Notably, the inhibition of ferroptosis using either drugs or genetic manipulation^{13,14} confers chemo-resistance in cancer cells suggesting that promoting ferroptosis would sensitize tumors to cytotoxic therapeutics.

Lipocalin 2 (LCN2) is a secreted glycoprotein^{15,16} that maintains the integrity of the gastrointestinal mucosa.¹⁷ LCN2 forms a complex with bacterial and human siderophores,¹⁵ thereby inhibiting bacterial growth and regulating iron homeostasis. Iron-bound LCN2 is imported into cells by complex formation with the LCN2 receptors, SLC22A17, MCR4 and LRP2.^{15,18} LCN2 binds to and protects the matrix-

metalloprotease-9 (MMP9) from auto-degradation with a concomitant increase in MMP9 activity.¹⁹ LCN2 is overexpressed in multiple tumor types,²⁰ including CRC,^{15,21} and is an indicator of colon cancer progression from adenoma to carcinoma.^{22–24} LCN2 over-expression leads to increased tumor formation in xenograft models of colon cancer.²³ We previously demonstrated that LCN2 is required to increase invasion and tumor progression observed upon plakophilin3 (PKP3) loss in the colon cancer cell line HCT116.²⁵ This report indicates that increased LCN2 levels correspond with an increase in resistance to 5FU. The resistance is dependent on the ability of LCN2 to inhibit ferroptosis by sequestering iron and stimulating the expression of xCT and GPX4. Finally, inhibiting LCN2 function with a monoclonal antibody sensitizes cells to therapy and inhibits tumor growth in xenograft mouse models.

2 | MATERIALS AND METHODS

2.1 | Patient samples

Tumor samples of 80 colon cancer patients were obtained from the ACTREC and TMH tissue repositories. A pathologist analyzed Hematoxylin and Eosin stained slides to confirm the presence of normal and tumor tissue.

2.2 | Plasmids and constructs

The LCN2 shRNA constructs have been previously described.²⁵ The oligonucleotides used to generate the xCT, and ETS1 shRNA constructs (Table S1) were cloned downstream of the U6 promoter in pLKO1.puro and pLKO.1hygro, respectively.

2.3 | Cell lines and transfections

HCT 116 cells (RRID:CVCL_0291) were obtained from Dr. Bert Vogelstein; HT-29 (RRID:CVCL_0320) and DLD-1 (RRID:CVCL_0248)

were obtained from Dr. Sanjeev Galande. Cell line authentication was performed using short tandem repeat profiling within the last 3 y and cultured as described.²⁵⁻²⁷ All experiments were performed with mycoplasma-free cells. Additional details are in Supplementary Materials and Methods.

2.4 | Chemicals

N-acetyl-L-Cysteine (catalog number A-7250, Sigma), erastin (catalog number E-7781, Sigma), RSL3 (catalog number SML2234, Merck), liproxstatin (catalog number SML-1414, Sigma), FER (catalog number SML-0583, Sigma), Z-VADFMK (catalog number SC-3067, Sigma), necrostatin (NEC) (catalog number CAS 4311-88-0, Sigma) and Catechol (catalog number C-9510, Sigma).

2.5 | Clonogenic survival assays

10³ cells were seeded into 35 mm cell culture plates and allowed to attach overnight. Cells were either pre-treated with the vehicle control or 5FU in combination with compounds such as N-acetyl cysteine (NAC), FER, NEC, LIP, Z-VADFMK, RSL3 and erastin, for 48 h. Similarly, cells treated with the vehicle control or 5FU were incubated with antibodies (3D12B2 and mIgG) or recombinant LCN2 proteins. Additional details are provided in the Supplementary Methods.

2.6 | Soft agar assays

Soft agar colony formation assays were performed in triplicate as described.²⁵ The results shown are an average of three independent experiments.

2.7 | Isolation of total RNA and real-time PCR reactions

The forward and reverse oligonucleotides used in our study are shown in Table S2. Quantitative reverse transcriptase PCRs were performed as described,²⁵ and GAPDH levels were used for normalization in all experiments.

2.8 | Antibodies and Western blot analysis

Protein extracts were prepared either in EBC lysis buffer (120 mM NaCl, 50 mM Tris-HCL (pH 8), 0.5% NP40 and protease inhibitors [5 µg/mL Leupeptin, 10 µg/mL Aprotinin, 0.2 mM sodium orthovanadate and 100 mM sodium fluoride])²⁸ or in 1X sample buffer as described.²⁹ Acetone precipitation of cell supernatants and Western blots were performed as described.²⁵ The anti-LCN2 antibody, 3D12B2, was generated and purified as described in

Supplementary Methods. Antibody dilutions are shown in Table S3. The blots were developed using Supersignal West Pico Chemiluminescent Substrate (Pierce), Super Signal West Femto Chemiluminescent Substrate (Pierce) and Clarity Western ECL substrate (Bio-Rad) as per the manufacturer's instructions. Where indicated blots were stripped using the Restore reagent (Pierce).

2.9 | Total reactive oxygen species (ROS) detection using CellROX or DCFDA

Oxidative stress was detected with the fluorogenic CellROX orange kit (Thermo Fisher Scientific, Inc.) or a DCFDA Cellular ROS Detection Assay Kit, Abcam (ab113851), as per the manufacturer's instructions. Additional details are provided in Supplementary Methods.

2.10 | Lipid ROS detection using BODIPY C11

BODIPY C11 was used to detect lipid ROS as per the manufacturer's instructions. Additional details are provided in the Supplementary Methods.

2.11 | Detection of ferric and ferrous iron

Ferric and ferrous iron were detected in the cells using an iron assay kit (Abcam) as per the manufacturer's instructions.

2.12 | Determination of GSH levels

GSH levels were determined by the Promega GSH-Glo Glutathione Assay kit as per the manufacturer's instructions. Additional details are provided in the Supplementary Methods.

2.13 | Chromatin immunoprecipitation

Cell lines were grown to 80%-90% confluence in 10 cm culture dishes. The oligonucleotides used for the chromatin immunoprecipitation experiments are in Table S4. Additional details are in the Supplementary Methods.

2.14 | Tumor formation in nude mice

6-8-wk-old CD1 Nude mice (CrI: CD1-Foxn1^{nu}) provided by the ACTREC laboratory animal house facility were used for the study. A controlled environment was provided to the animals with a temperature of 22°C ± 2°C, and relative humidity was maintained at 40%-70%. A 12 h day-night cycle was maintained (7:00 to 19:00 day and 19:00 to 7:00 night). The animals were given a gamma-irradiated

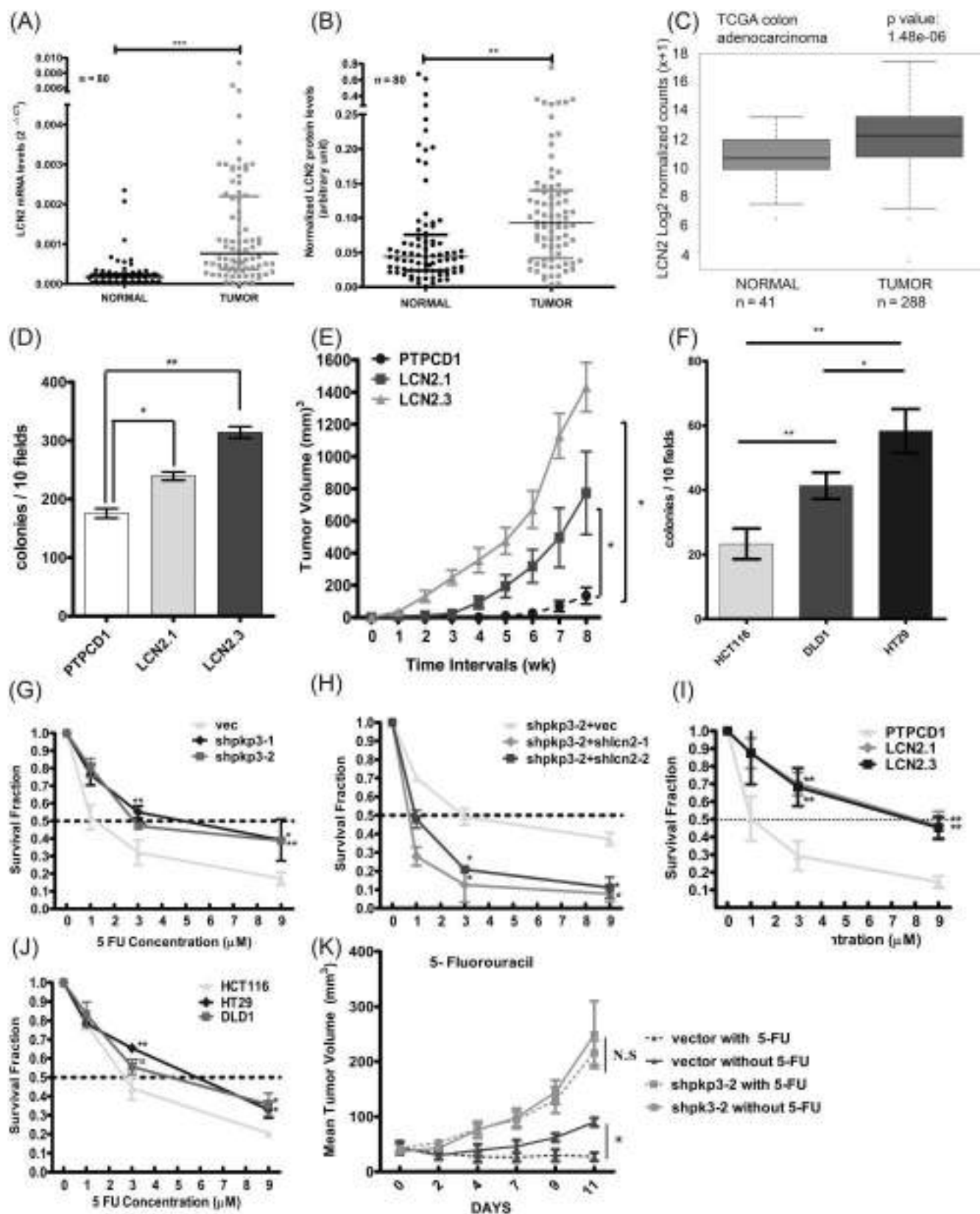


FIGURE 1 Legend on next page.

balanced diet (Altromin International 1314P) and sterile water *adlibitum*. Individually ventilated Cage system (IVC, M/S Citizen, India) was used to house mice used in the experiments. These IVCs were provided with autoclaved corn cob as bedding for the mice. Animal euthanasia was done using CPCSEA recommended euthanizing agent, carbon dioxide. Immunocompromised mice were injected subcutaneously in the dorsal flank with 1×10^6 cells of the HCT116 derived vector control (vec) or PKP3 knockdown clone (shpkp3-2) or 1×10^7 DLD1 cells. Once the DLD1 tumors grew, the mice were sacrificed, and 3 mm³ tumor pieces were transplanted into NOD SCID (NOD.CB17-Prkdcscid/NcrCrI) mice. Tumor formation and volume were monitored. Once the tumors reached a specific size (about 50–100 mm³), the mice were either injected with the vehicle control (PBS) or 30 mg/kg 5-FU (IP) thrice a week for 2 wk. Where indicated, 100 µg of mouse immunoglobulin G (mIgG) or 3D12B2 was injected IV every week. Tumor volume was determined using vernier calipers using the formula $(0.5 \times LV^2)$, where L is the largest dimension and V is the perpendicular dimension. The mean tumor volume and SEM are were plotted on Y-axis, and the number of days was plotted on X-axis. P -values were obtained using the student's t -test.

2.15 | Statistical analysis

Data for in vitro experiments are represented as mean and SD from three independent experiments. For in vivo experiments, it is represented as mean and SEM. Statistical significance for adjacent normal and tumor tissue samples (real-time and Western blot quantitation) and in-vivo experiments was calculated using paired t test. The P -value for TCGA colorectal adenocarcinoma was calculated using Wilcoxon-Mann-Whitney test analysis. Statistical significance for the remaining experiments was determined by conducting an unpaired t test. Data were considered significant for P -value $< .05$. GraphPad (v7) was used to generate the boxplot, bar-graphs and scatter dot plots.

2.16 | Analysis of TCGA data

RNAseq gene expression, normalized $(\log_2X + 1)$ counts for TCGA colon adenocarcinoma (PanCancer Atlas) were obtained from UCSC xena (<https://xenabrowser.net/datapages/?dataset=TCGA.COAD.sampleMap%2FHiSeqV2&host=https%3A%2F%2Ftcga.xenahubs.net&removeHub=http%3A%2F%2F127.0.0.1%3A7222>). As per TCGA bar code, normal and tumor samples were distributed, and R 3.3.3 software (<http://www.R-project.org/>) was used for box plot representation. P -value was calculated using the Wilcoxon-Mann-Whitney test analysis.

2.17 | Pearson's correlation analysis

Colorectal adenocarcinoma (TCGA, firehose legacy [provisional data]) cohort was selected from cBioPortal, and mRNA expression z-scores relative to diploid sample (RNA seq V2 RSEM) were used to find the Pearson's r (correlation coefficient) with cut-off value of 1.5. P -value was calculated using t -distribution.^{30,31}

2.18 | Ethics statement

Animals were maintained in the ACTREC animal house facility following the national guidelines mentioned by the Committee for the Purpose of Control and Supervision of the Experiments on Animals (CPCSEA), Ministry of Environment, Forest and Climate Change, Government of India. The Institutional Animal Ethics Committee (IAEC) of the Advanced Centre for Treatment Research and Education in Cancer (ACTREC) approved all the protocols used in this report. The project number for the study is 30/2016.

For human tumor samples, study number 124 was approved by the Institute Ethics Committee III (IEC III) ACTREC, Tata Memorial Centre (TMC) on 28 October 2013. A waiver of consent was

FIGURE 1 LCN2 expression is associated with increased tumor progression and therapy resistance. A, mRNA was purified from 80 matched colon tumor and normal paired tissue samples. qRT-PCR reactions for LCN2 were performed and normalized to GAPDH levels and the $2^{-\Delta CT}$ values from normal and tumor samples were plotted. Horizontal bars show the median value of LCN2 levels. B, Protein extracts from matched normal and tumor samples were resolved on SDS-PAGE gels and Western blots performed for LCN2. The mean intensity of the LCN2 band was normalized to the total protein levels, as determined by staining the blot with Ponceau-S and the normalized value plotted. Horizontal bars show the median value of intensity. C, TCGA data analysis of LCN2 in COAD (TCGA colon cancer) ($n = 288$) and cut margin samples ($n = 41$), represented as $(\log_2x + 1)$. Note that the LCN2 levels are high in the tumor samples as compared to the normal tissue. D, Soft agar colony formation assays were performed with the indicated cell lines. The number of colonies per 10 fields was measured, and the mean and SD are plotted on the Y-axis. E, 10^6 cells of the HCT116 derived LCN2 overexpressing clones LCN2.1 and LCN2.3 or the vector control were injected into immunocompromised mice, and tumor volume was monitored for 8 wk. The mean and SEM is plotted. F, Soft agar colony formation assays were performed with the indicated cell lines. The number of colonies per 10 fields was measured, and the mean and SD are plotted on the Y-axis. Note that increased LCN2 levels correlate with an increase in colony number. G–J, The indicated cell lines were treated with different concentrations of 5FU, and clonogenic survival assays were performed. The mean and SD of the survival fraction at different doses of 5FU is plotted. The horizontal line represents the IC_{50} for each cell line. K, Immunocompromised mice were injected subcutaneously in the dorsal flank with 1×10^6 cells of the HCT116 derived vector control (vec) or PKP3 knockdown clone (shpkp3-2). Once the tumors reached a specific size (30–50 mm³), mice were either injected with the vehicle control (PBS) or 30 mg/kg 5-FU (IP) thrice a week for 2 wk. Where indicated, the P -value was determined by the student's t -test (** $P < .001$, ** $P < .01$, * $P < .05$)

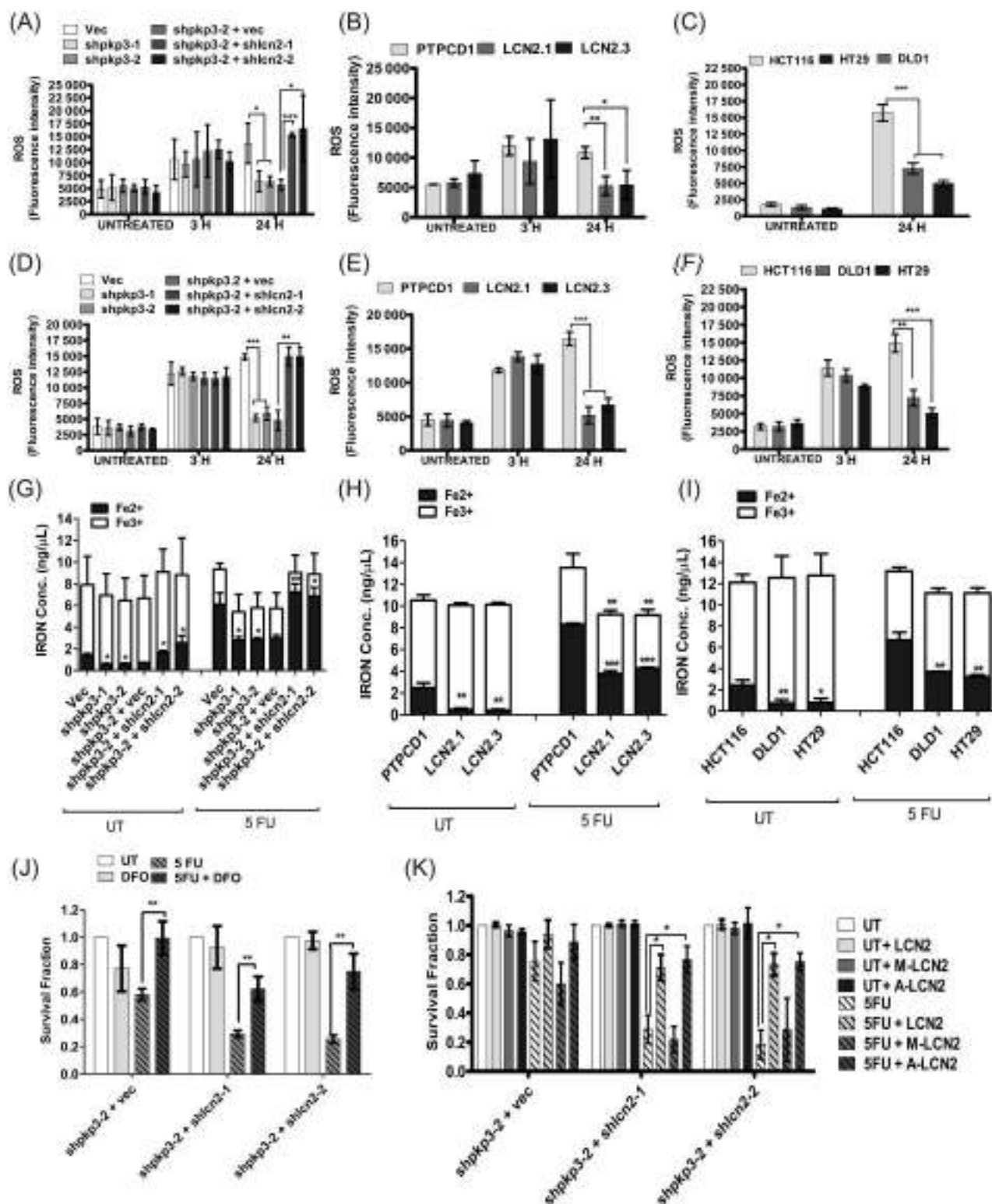


FIGURE 2 LCN2 expression leads to ROS clearance and is dependent on the ability of LCN2 to bind iron. A-F, The levels of total ROS were determined using DCFDA (A-C) and CellROX (D-F). The indicated cell lines were incubated in the presence or absence of 5FU for the indicated times, and fluorescence intensity was measured. The mean and SD are plotted on the Y-axis. G-I, The indicated cell lines were untreated or treated with 5FU for the indicated time points and cellular iron levels measured. The mean and SD are plotted. J, The indicated cell lines were treated with the vehicle control or with deferoxamine (DFO), and survival assays were performed. The mean and SD of the survival fraction is plotted on the Y-axis. K, The indicated cell lines were seeded and then pre-treated with either the vehicle control, recombinant WT LCN2 (LCN2), ApoLCN2 (A-LCN2), or a mutant LCN2 that does not bind iron (M-LCN2) for 12 h, followed by treatment with 3 μ M 5FU for 48 h. The survival fraction is plotted on the Y-axis. The mean and SD is plotted. Where indicated *P*-values were determined using a student's *t* test. (**P* < .05, ***P* < .01, ****P* < .001 and ns = not significant)

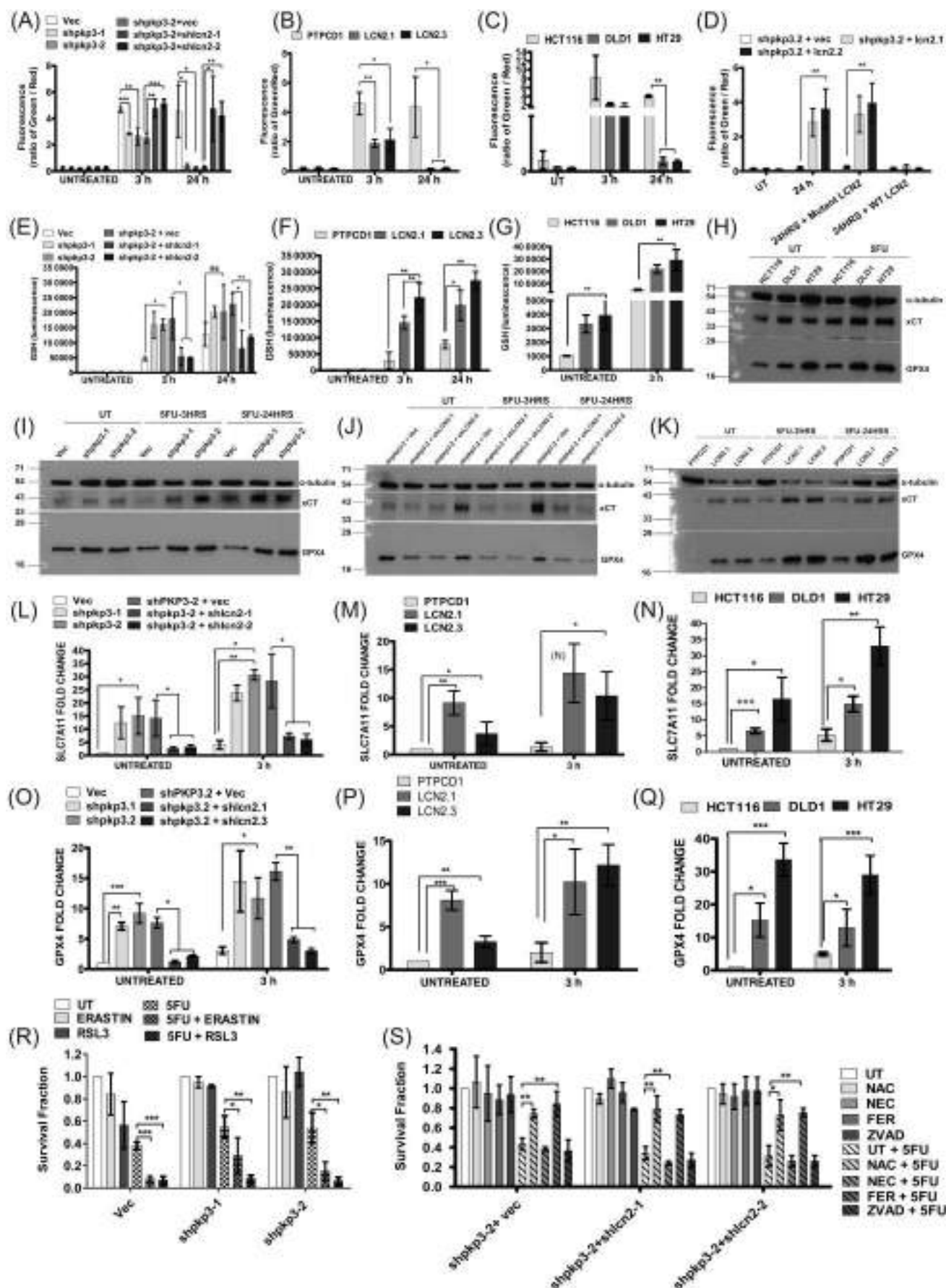


FIGURE 3 Legend on next page.

requested and granted for samples obtained from the Tata Memorial Hospital (TMH) and ACTREC tumor repositories.

3 | RESULTS

3.1 | LCN2 levels are increased in colon cancer and lead to an increase in resistance to 5FU

LCN2 mRNA and protein levels were measured by quantitative reverse transcriptase coupled PCR (qRT-PCR) and Western blot analysis, respectively, in 80 matched normal and colon cancer samples collected at the Tata Memorial Centre (TMC). LCN2 mRNA and protein levels were substantially elevated in tumor tissues compared to adjacent morphologically normal tissue (Figures 1A-B and S1A-B). Similarly, LCN2 mRNA expression was elevated in the TCGA colon adenocarcinoma (COAD) dataset (Figure 1C). These results suggest that LCN2 expression is elevated in colon tumor samples.

Loss of PKP3 in the colon cancer cell line HCT116 led to an increase in secreted LCN2 expression, which was required for tumor progression.²⁵ In addition to this model (Figure S1C), we generated LCN2 over-expressing lines in HCT116 cells (Figure S1D,F) and determined LCN2 secreted protein and mRNA levels in different CRC cell lines (Figure S1E,G). Overexpression of LCN2 in HCT116 cells led to an increase in colony formation in soft agar (Figures 1D and S1H) and tumor formation in immunocompromised mice (Figures 1E and S1I). Similarly, an analysis of the different colon cancer lines demonstrated that increased LCN2 expression correlated with an increase in colony number in soft agar assays (Figures 1F and S1J).

Clonogenic survival assays demonstrated that PKP3 loss led to increased resistance to 5FU (Figure 1G). The observed resistance was dependent on LCN2 expression as the double knockdown clones showed increased sensitivity to 5FU (Figure 1H). Similar results were observed when the LCN2 over-expressing clones were treated with 5FU (Figure 1I). Similarly, increased resistance to 5FU correlated with increased LCN2 levels in the different colon cancer cell lines tested (Figure 1J). To determine if the increase in resistance was observed in vivo, the vector control or the PKP3 knockdown clones were injected into immunocompromised mice and treated with 5FU when the

tumors reached a specific size. The vector control responded to the treatment with 5FU, and tumor size regressed while the PKP3 knockdown clones continued to grow in size (Figures 1K and S1K). These results suggest that LCN2 is both necessary and sufficient for the resistance to 5FU.

3.2 | LCN2 expression leads to the clearance of ROS

LCN2 may promote resistance to 5FU by increasing ROS clearance. Cells were untreated or treated with 5FU, and ROS clearance was measured post-treatment in two different assays. While all cells had similar ROS levels at 3 h post-treatment, the PKP3 knockdown clones showed increased ROS clearance 24 h post-treatment than the vector controls in both assays (Figure 2A,D). In contrast, the PKP3 LCN2 double knockdown clones could not clear ROS 24 h post-treatment (Figure 2A,D). Similarly, increased LCN2 levels correlated with ROS clearance in the LCN2 overexpressing clones (Figure 2B,E) and the different colon cancer cell lines (Figure 2C,F).

The levels of ferrous (Fe^{2+}) and ferric (Fe^{3+}) iron regulate the production of ROS due to a combination of the Haber Weiss reaction and the Fenton reaction.¹⁵ LCN2 binds to Fe^{3+} in the presence of catechol and prevents the conversion of Fe^{3+} to Fe^{2+} , thus breaking the cycle of ROS generation leading to clearance of ROS³² (Figure S2A). Consistent with these observations, the total iron levels were reduced in the PKP3 knockdown cells post-treatment with 5FU compared to the vector control or the PKP3+LCN2 double knockdown cells (Figure 2G). Interestingly, the double knockdown cells had higher intracellular iron levels even in the absence of any treatment. Most of the iron in the untreated cells was in the ferric form. After treatment with 5FU, the ferrous form was more abundant. (Figure 2G). However, the total iron and ferrous iron levels were much lower in the PKP3 knockdown cells than the vector control and the double knockdown cells. Catechol levels were unchanged in these cells upon treatment with 5FU (Figure S2B,C). Upon treatment with 5FU, the levels of ferrous iron were much lower in the HCT116 derived LCN2 over-expressing cells (Figure 2H) and in the HT29 and DLD1 cells as compared to HCT116, which is consistent with the difference observed in

FIGURE 3 LCN2 inhibits ferroptosis by promoting the expression of xCT and GPX4. A-D, The indicated cell lines were untreated or treated with 5FU for the indicated time points. The levels of lipid ROS were measured using C11 BODIPY dye (10 μM). The green to red ratio was determined, and the mean and SD are plotted on the Y-axis. Where indicated recombinant WT or mutant LCN2 proteins were added to the media before treatment with 5FU. E-G, The indicated cell lines were untreated or treated with 5FU for the indicated time points, and GSH levels were determined. The mean fluorescent intensity was determined, and the mean and SD are plotted on the Y-axis. H-K, The indicated cell lines were untreated or treated with 5FU for the indicated time points, and protein extracts were prepared as described. 100 μg of protein extracts was resolved on 12% SDS PAGE gels followed by Western blotting with the indicated antibodies. Note that cell lines with elevated LCN2 levels correlated with an increase in xCT and GPX4 levels. α tubulin served as a loading control. L-Q, xCT (L-N) and GPX4 (O-Q) mRNA levels were determined by qRT-PCR in the indicated cell lines. The fold change was determined, and the mean and SD are plotted on the Y-axis. R, The indicated cell lines were untreated or treated with 5FU in combination with the ferroptosis promoters erastin or RSL3, and clonogenic survival assays were performed. The mean and SD of three different experiments are plotted. S, The indicated cell lines were untreated or treated with 5FU or 5FU in combination with either of N-Acetyl-L-Cysteine (NAC), Necrostatin (NEC), Ferrostatin (FER) and Z-VADFMK (ZVAD), and survival assays were performed. The mean and SD are plotted on the Y-axis. Unless otherwise indicated *P*-values were obtained using a student's *t* test (**P* < .05, ***P* < .01, ****P* < .001 and ns = not significant)

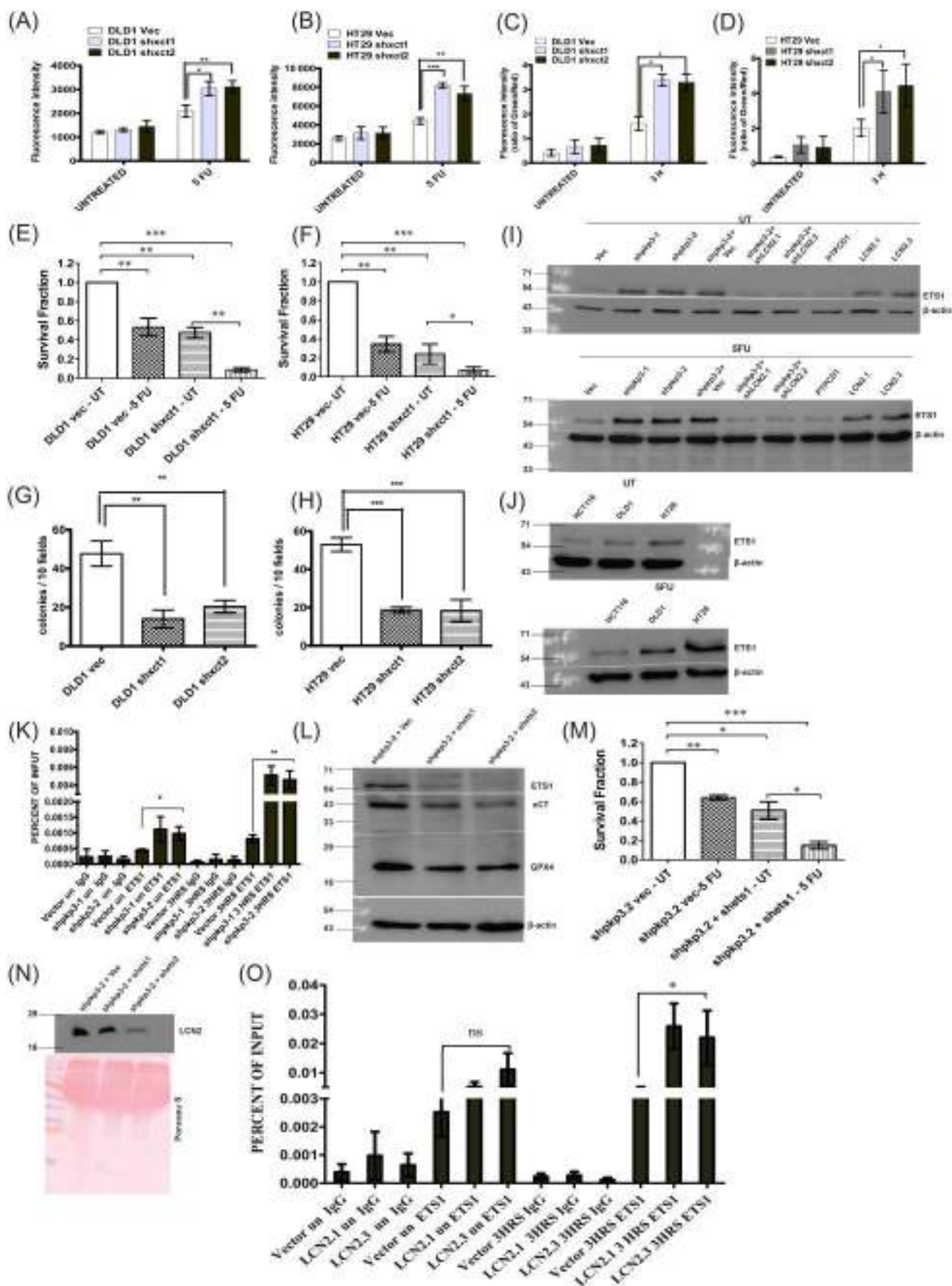


FIGURE 4 Legend on next page.

LCN2 levels in these cell lines (Figure 2H,I). Consistent with these results, treating the PKP3 LCN2 double knockdown clones with the iron chelator, deferoxamine (DFO), resulted in increased cell survival upon treatment with 5FU (Figure 2J). To determine if the ability of LCN2 to bind the iron catechol complex was required for the resistance to 5FU, the PKP3+LCN2 double knockdown cells were incubated with recombinant forms of HoloLCN2 (iron-bound), ApoLCN2 (not bound to iron), and an LCN2 mutant (K125AK134A), which cannot bind to the iron catechol complex (³² and Figure S2A), before treatment with 5FU. Treatment with the recombinant Holo and Apo LCN2 proteins resulted in increased survival of the double knockdown clones. In contrast, the K125AK134A mutant could not confer resistance to 5FU (Figure 2K). These results suggested that the ability of LCN2 to bind the iron-catechol complex is required to stimulate clearance of ROS.

3.3 | LCN2 inhibits ferroptosis by stimulating GSH production and clearing peroxidated lipids

The results above showed that increased LCN2 expression leads to decreased intracellular levels of ferrous iron. Increased ferrous iron levels are a feature of ferroptosis.⁴ Peroxidated lipids accumulate during ferroptosis, and the level of LCN2 expression correlated with the increased clearance of peroxidated lipids upon treatment with 5FU (Figure 3A-C). In contrast, a knockdown of LCN2 in the PKP3 knockdown clones impaired the clearance of peroxidated lipids (Figure 3A). Treatment of the PKP3 LCN2 double knockdown clones with recombinant WT LCN2 led to an increased clearance of lipid ROS. In contrast, treatment with the K125AK134A mutant did not restore the ability to clear peroxidated lipids (Figure 3D), indicating that the ability of LCN2 to stimulate the clearance of peroxidated lipids was

dependent on its ability to bind the iron-catechol complex. These results suggest that the clearance of lipid ROS by LCN2 is dependent on the ability of LCN2 to regulate iron homeostasis.

The increase in peroxidated lipids is due to a decrease in either the levels of GPX4 or a reduction in intracellular GSH levels due to the inhibition of system x_c^- .^{4,5,7} We demonstrated that the levels of LCN2 correlated with an increase in the levels of GSH in all the cell lines (Figure 3E-G). Inhibition of LCN2 expression in the PKP3 knockdown clones led to decreased GSH levels (Figure 3E). To determine if increased GSH levels were due to an increase in the levels of either GPX4 or system x_c^- , we demonstrated that the protein and mRNA levels of the transport subunit of system x_c^- , xCT (gene name *SLC7A11*) or GPX4 were higher in cells with high levels of LCN2 especially post-treatment with 5FU (Figure 3H-K and Figure 3L-Q). Though xCT and GPX4 levels increased in all the cell lines upon treatment with 5FU, the increase was more significant in cell lines expressing higher levels of LCN2. In contrast, a knockdown of LCN2 in the PKP3 knockdown cells led to a decrease in xCT levels upon 5FU treatment (Figure 3J, L, O).

Treatment with the ferroptosis inducers, erastin and RSL-3,^{7,10,11} led to a decrease in survival in cell lines with high levels of LCN2 (Figure 3R). To determine if the reduction in survival in the presence of 5FU had contributions from other cell death pathways, different CRC lines and PKP3+LCN2 double knockdown clones were treated with the IC₅₀ of 5FU in the presence or absence of vehicle control, an apoptosis inhibitor (ZVAD), a necroptosis inhibitor NEC, a ferroptosis inhibitor FER and the cell-permeable cysteine analogue, NAC. Treatment with ZVAD or NEC did not significantly increase cell survival in 5FU compared to the vehicle control (Figures 3S and S3A-C). In contrast, treatment with either FER or NAC led to a significant increase in survival in the presence of 5FU (Figures 3S and S3A-C). Similarly, treatment with the ferroptosis inhibitor LIP in the presence or absence of 5FU led to increased

FIGURE 4 Loss of xCT or *ETS1* leads to a reversal of therapy resistance in cells expressing LCN2. A-B, Stable cell lines expressing the vector control or shRNAs targeting xCT were generated in DLD1 (DLD1+vec, DLD1+shxct1 and DLD1+shxct2) (A) and HT29 (HT29+vec, HT29+shxct1, HT29+shxct2) (B) were untreated or treated with 5FU and ROS levels measured using DCFDA. The mean fluorescent intensity was determined, and the mean and SD plotted on the Y-axis. C-D, The levels of lipid ROS were measured using C11 BODIPY dye in the indicated cell lines. The mean and SD of the ratio of green to red fluorescence was plotted on the Y-axis. E-F, The indicated cell lines were untreated or treated with 5FU, and the survival fraction was determined. The mean and SD are plotted. G-H, Soft agar assays were performed in the indicated cell lines and the number of colonies per 10 fields determined. The mean and SD is plotted on the Y-axis. I-J Protein extracts were prepared from the indicated cell lines that were untreated or treated with 5FU. The extracts were resolved on SDS-PAGE gels followed by Western blots with antibodies to *ETS1*. Note that *ETS1* levels are higher in cells expressing LCN2 and are further stimulated upon 5FU treatment. Western blots for β actin served as a loading control. K, ChIP assays were performed using either a non-specific rabbit IgG (IgG) or *ETS1* antibodies from the indicated cell lines that were untreated or treated with 5FU, followed by qPCR to detect the xCT promoter. The mean and SD are plotted. L, *ETS1* expression was inhibited in the indicated cell lines with two different shRNA constructs. Protein extracts were prepared, and 100 μ g of the lysates were resolved on 12% SDS PAGE gels followed by Western blotting with antibodies specific to *ETS1*, xCT and GPX4. Western blots for β actin served as a loading control. The samples for the actin blot were run in a parallel set of lanes on the same gel. Note that a decrease in *ETS1* levels leads to a decrease in xCT and GPX4 levels. M, *ETS1* expression was inhibited in the indicated cell lines with two different shRNA constructs, and survival assays were performed in the presence and absence of 5FU and the survival fraction determined. The mean and SD is plotted. N, 200 μ g of acetone precipitated cell supernatants was prepared from the indicated cell lines and resolved on 12% SDS PAGE gels followed by Western blotting with antibodies specific to LCN2. The same blot was stained with Ponceau to serve as a loading control. Note that LCN2 levels are decreased upon a decrease in *ETS1* levels. O, ChIP assays were performed using either a non-specific rabbit IgG (IgG) or *ETS1* antibodies from the indicated cell lines that were untreated or treated with 5FU, followed by qPCR to detect the LCN2 promoter. The mean and SD are plotted. Where indicated *P*-values were determined using a student's *t* test. (**P* < .05, ***P* < .01, ****P* < .001 and ns = not significant) [Color figure can be viewed at wileyonlinelibrary.com]

resistance to 5FU in the LCN2 PKP3 double knockdown clones as compared to the vehicle control (Figure S3D).

xCT expression was inhibited using vector-driven RNAi in cells with high LCN2 levels; the HCT116 derived PKP3 knockdown clones and the colon cancer cell lines, HT29 and DLD1. Stable lines with a knockdown of xCT were generated (Figure S3E-J). Loss of xCT leads to an increase in the levels of total ROS (Figures 4A-B and S3K) and

peroxidated lipids (Figures 4C-D and S3L) upon treatment with 5FU. xCT knockdown also led to a decrease in survival in the presence and absence of 5FU (Figures 4E-F and S3M) and reduced colony formation in soft agar (Figures 4G-H and S3N). These results suggest that the increase in LCN2 expression leads to an inhibition of ferroptosis induced by 5FU due to alterations in intracellular iron levels and increased system x_c⁻ activity.

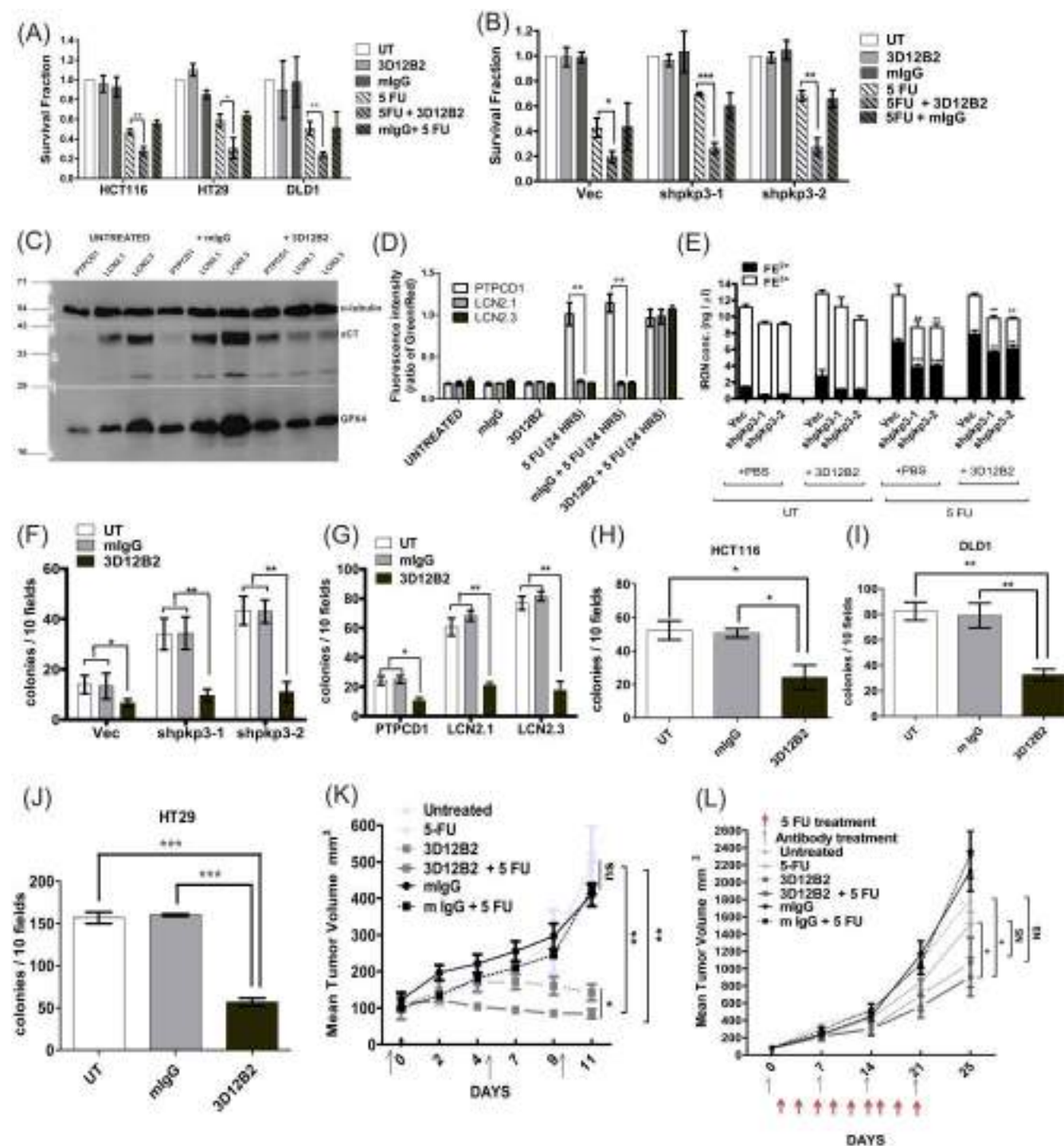


FIGURE 5 Legend on next page.

3.4 | LCN2 induces xCT expression by stimulating ETS1 expression

Multiple transcription factors, including *ETS1*, *ATF4* and *NRF2*, regulate xCT expression.^{33–35} An *in silico* analysis using JASPAR software identified multiple *ETS1* binding sites in the *SLC7A11* promoter (Figure S4A). LCN2 expression led to increased *ETS1* mRNA levels in the HCT116 derived PKP3 knockdown clones and LCN2 over-expressing clones (Figure S4B–C). LCN2 expression led to increased *ETS1* protein levels in all the cell lines tested (Figure 4I–J) in the presence or absence of 5FU. Similarly, loss of LCN2 in either the PKP3 KD cells (Figure 4I–J) or in the HT29 and DLD1 cells (Figure S4J) led to a decrease in *ETS1* levels. Chromatin immunoprecipitation (ChIP) assays followed by real-time PCR demonstrated that *ETS1* showed a higher occupancy at the xCT promoter in cell lines with elevated LCN2 levels than the respective vector controls, especially upon treatment with 5FU (Figures 4K and S4D).

To further confirm these results, we transiently inhibited *ETS1* expression in the PKP3 knockdown clones and in HT29 cells, both of which have high LCN2 levels (Figures 4L and S4E–G). xCT and GPX4 levels decreased in the *ETS1* knockdown clones (Figures 4L and S4G). Treatment of these cells with 5FU led to a decrease in survival (Figures 4M and S4H), and LCN2 expression also decreased upon *ETS1* knockdown (Figures 4N and S4I), suggesting the presence of a positive feedback loop between the two genes. CHIP assays demonstrated increased occupancy of the LCN2 promoter by *ETS1* in the presence of 5FU with a smaller but not significant increase in occupancy in the absence of 5FU (Figure 4O). These results suggest that LCN2 stimulates an increase in the transcription factor *ETS1*, leading to increased xCT expression.

3.5 | Inhibiting LCN2 function leads to sensitivity to 5FU *in vitro* and *in vivo*

We generated a specific monoclonal antibody to LCN2 (3D12B2) and confirmed the specificity by performing Western blots in cells with

low and high levels of LCN2 or an LCN2 knockdown (Figure S5A–B). The different colon cancer lines were incubated with either the vehicle control, mIgG, or 3D12B2 for 12 h before adding the IC₅₀ value of 5FU followed by survival assays. Treatment with the antibody but not mIgG or the vehicle control resulted in a significant decrease in survival in response to 5FU treatment (Figure 5A). Similar results were obtained in the HCT116 derived PKP3 knockdown cells (Figure 5B). Treatment with 3D12B2 but not the control antibody led to a decrease in the levels of xCT and GPX4 (Figures 5C and S5C–D), a reduction in *ETS1* levels (Figure S5E) and a decrease in the clearance of peroxidated lipids (Figure 5D). Treatment with 3D12B2 led to an increase in the intracellular levels of ferrous iron, especially upon treatment with 5FU as compared to the vehicle control (Figure 5E). Treatment with 3D12B2 led to decreased colony formation in soft agar compared to treatment with mIgG in all cells (Figures 5F–J and S5F–J).

Nude mice were injected with the PKP3 knockdown clones or the DLD1 cell line. Once the tumors grew to the appropriate size, they were either untreated or treated with 5-FU as described. In addition to 5-FU treatment, nude mice were also injected with either the vehicle control, non-specific mIgG, or 3D12B2, and tumor volume monitored. Tumors formed efficiently in mice injected with the PKP3 knockdown clones or the DLD1 cells in the presence or absence of 5FU (Figure 5K–L). Treatment with the non-specific mIgG did not affect tumor formation. In contrast, treatment with 3D12B2 inhibited tumor progression and induced tumor regression in combination with 5FU in the PKP3 knockdown clones (Figure 5K). Treatment with 3D12B2 led to a significant decrease in tumor growth in mice injected with the DLD1 cells, with a further reduction in growth in the presence of 5FU (Figure 5L). The different treatments had no significant effects on body weight (Figure S5K–L). These results suggest that 3D12B2 could be a potential molecule for tumor therapy.

The results described above suggest that LCN2 inhibits ferroptosis by regulating intracellular iron levels and promoting the expression of *ETS1*, leading to an increase in the levels of xCT and GPX4. To further extend these studies, we determined xCT levels in colon tumor samples and the adjacent normal tissue. qRT-PCR

FIGURE 5 Inhibiting LCN2 function inhibits chemoresistance and tumor progression. A–B, The indicated cell lines were treated with 5-FU or the vehicle control in the presence of vehicle control, non-specific mouse IgG (mIgG), or 3D12B2, and survival fractions were determined. The mean and SD are plotted. Note that treatment with 3D12B2 results in an increase in sensitivity to 5FU in LCN2 expressing cells. C, The indicated cell lines were treated with mIgG or 3D12B2 in the presence or absence of 5FU, and protein extracts resolved on SDS-PAGE gels followed by Western blotting with the indicated antibodies. D, The indicated cell lines were treated with 3D12B2 or the vehicle control (PBS) in the presence or absence of 5FU, and the levels of peroxidated lipids were determined. The mean and SD are plotted. E, HCT116 derived vector control and PKP3 knockdown clones were untreated (UT) or pre-treated with 3D12B2 for 12 h, followed by treatment with either the vehicle control or 5FU for 3 h. The cells were harvested, and the levels of total iron, ferric and ferrous iron levels were determined, and the mean and SD plotted on the Y-axis. F–J, Soft agar assays were performed in the indicated cell lines in the presence of the vehicle control (UT), non-specific mouse IgG (mIgG), or 3D12B2, and the number of colonies in 10 low power fields determined in triplicate. The mean and SD was plotted. K–L, 10⁶ cells of the HCT116 derived PKP3 knockdown clone (shpkp3-2) (K), or a piece of a tumor formed by the DLD1 cell line (L) was injected subcutaneously on the mouse flank. Once the tumors reached a size of 100 mm³, mice were either injected with the vehicle control (PBS) or 30 mg/kg 5-FU (IP) thrice a week for 2 wk in the presence of either the vehicle control, non-specific mouse IgG (mIgG) or 3D12B2 (100 µg IV). The arrows indicate the time of injection. Tumor volume was determined as described. The mean tumor volume and SEM are plotted on the Y-axis. Note that treatment with 3D12B2 results in an inhibition of tumor growth, and treatment with both 3D12B2 and 5FU results in a reduction in tumor growth. Where indicated, *P*-values were determined using a student's *t* test (**P* < .05, ***P* < .01, ****P* < .001 and ns = not significant) [Color figure can be viewed at wileyonlinelibrary.com]

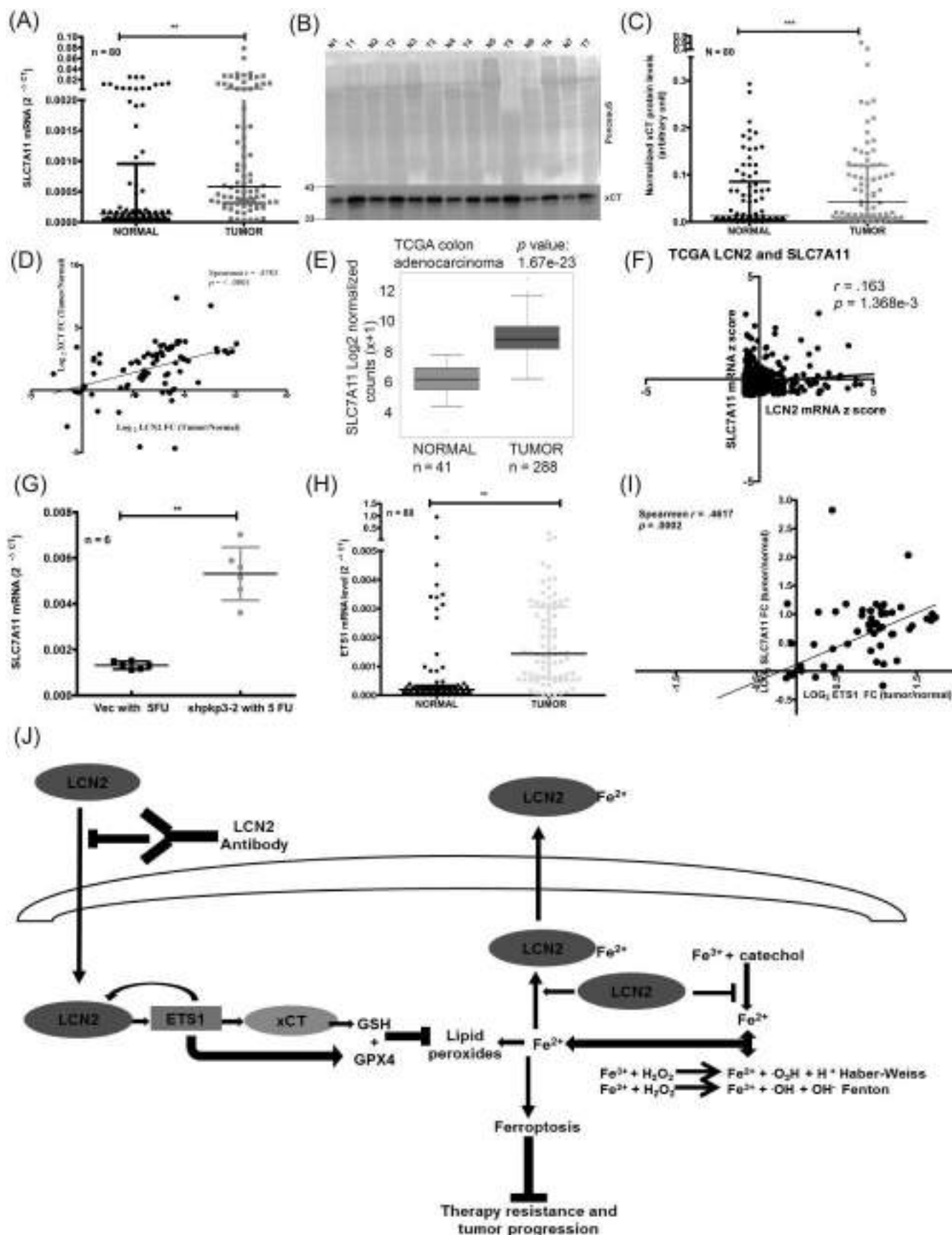


FIGURE 6 Legend on next page.

(Figure 6A) and Western blot analyses (Figure 6B-C) demonstrated that xCT levels were elevated in colon tumor samples as compared to adjacent normal tissue. A positive correlation was observed between the mRNA levels of LCN2 and xCT when analyzing the tumor samples used in our study (Figure 6D). A larger percentage of Stage T3 tumors had higher LCN2 and xCT protein levels than the adjacent normal (Figure S6A-B). A similar analysis on the COAD cohort from TCGA demonstrated that xCT levels were significantly increased in tumor samples compared to normal tissue (Figure 6E). A positive correlation was observed between the mRNA levels of LCN2 and xCT in the TCGA cohort (Figure 6F). An analysis of xCT levels in the tumor xenografts in immunocompromised mice that were treated with 5FU showed an increase in xCT expression in the tumors formed by the PKP3 knockdown clones than the vector control (Figure 6G). Similarly, *ETS1* mRNA levels significantly increased in colon tumor samples compared to the adjacent normal controls (Figure 6H) and showed a positive correlation with xCT levels (Figure 6I). These results suggest that the pathways underlying the increase in chemoresistance, as indicated by our cell line data, represent what might be happening in human tumor samples.

4 | DISCUSSION

The results in this report suggest that LCN2 expression leads to tumor progression and chemo-resistance in colon cancer cells. This is also consistent with data from human colon tumor samples, which have high LCN2 levels as compared to adjacent normal controls. These data are consistent with previous reports that LCN2 is over-expressed in colon tumors^{20,36} and some evidence that suggests that increased LCN2 levels are associated with poor survival.³⁷ LCN2 is an indicator of colon cancer progression from adenoma to carcinoma,²²⁻²⁴ and LCN2 over-expression leads to increased tumor formation in xenograft models of colon cancer.²³ In an APC^{min} mouse model, LCN2 expression inhibits tumor progression in the proximal tissue of the small intestine but is required for tumor progression in the distal region of the small intestine.³⁸ There is some evidence to suggest that while LCN2 expression is elevated in primary tumors and can lead to

tumor progression, LCN2 expression is negatively correlated with metastatic progression in CRC.^{39,40} Our results demonstrate that LCN2 is required for tumor progression in colon cancer cell lines and is elevated in colon tumor samples, and could be a relevant therapeutic target in CRC, especially therapy resistant colon cancer. However, only adjuvant chemotherapy comprising 5FU and Oxaliplatin is given to patients with Stages III and IV colon cancer¹ and as all the data in this report and the TCGA data set is generated from surgically resected samples, there is no data available on therapy resistance for these patients. However, as most of the patients with LCN2 levels greater than the adjacent normal tissue are at Stage III, it is possible that inhibiting LCN2 function in these tumors will lead to a further decrease in tumor burden in these patients.

LCN2 inhibits ferroptosis by regulating intracellular iron levels and by inducing the expression of xCT and GPX4. Inhibiting LCN2 function with the anti-LCN2 monoclonal antibody (3D12B2) results in an increase in ferrous iron in cells and a decrease in GPX4 and xCT expression, which promotes ferroptosis, leading to increased sensitivity to chemotherapy and a reduction in tumor formation. Loss of GPX4 in mice leads to severe toxicity and death of the animal,⁹ and while a loss of xCT is not lethal, it results in defects in spatial working memory.⁴¹ In contrast, the loss of LCN2 does not result in lethality in mice.⁴² Therefore, inhibition of LCN2 function in tumor cells could serve as a novel way of inducing ferroptotic cell death in tumors with minimal toxicity in normal tissues. Thus, LCN2 is a potential drug target in therapy-resistant CRC and other cancer types.²⁰ Further, as LCN2 is also over-expressed in other conditions such as age-related macular degeneration⁴³ and chronic kidney disease,⁴⁴ the 3D12B2 antibody could also serve as a potential therapeutic in these chronic conditions.

Previous reports suggest that CRCs show an increase in the levels of proteins required for iron import.⁴⁵ Excess iron contributes to tumor initiation and progression in humans,^{46,47} human CRC,⁴⁸ and mouse models of colon cancer.⁴⁹ Increased iron levels lead to ROS generation by iron via the Fenton and Haber-Weiss reactions,⁵⁰ and tumor progression in the colon is associated with increased ROS levels.^{51,52} In contrast, the results in this report indicate that excessive iron can lead to tumor cell killing through the amplification of ROS

FIGURE 6 LCN2 levels correlate with an increase in xCT levels in human tumor samples. A, mRNA was purified from 80 matched colon tumors and normal paired tissue samples. qRT-PCR reactions for xCT were performed and normalized to *GAPDH* levels and the $2^{-\Delta CT}$ values from normal and tumor samples were plotted. Horizontal bars show the median value of xCT levels. B-C, Protein extracts from matched normal and tumor samples were resolved on SDS-PAGE gels and Western blots performed for xCT. The mean intensity of the xCT band was normalized to the total protein levels, as determined by staining the blot with Ponceau-S, and the normalized value plotted. Horizontal bars show the median value of intensity (a.u.). D, Pearson's *r* analysis of *SLC7A11* and *LCN2*. Data represented as scatter plot where *r* and *P* correspond to the correlation coefficient and *P*-value, respectively. Note that there is a positive correlation between *LCN2* and *SLC7A11* levels. E, Boxplot representation of *SLC7A11* in COAD (TCGA colon cancer) (*n* = 288) and cut margin samples (*n* = 41), represented as ($\log_2 x + 1$). F, Pearson's coefficient analysis of *SLC7A11* and *LCN2* expression in the TCGA data set. The data are represented as a scatter plot where *r* and *p* refer to the correlation coefficient and *P*-value, respectively. Where indicated, *P*-values were determined using a student's *t* test. G, *SLC7A11* mRNA levels were measured in mRNA purified from tumor xenografts. Note that xCT expression is elevated in tumor samples. H, mRNA was purified from 80 matched colon tumors and normal paired tissue samples. qRT-PCR reactions for *ETS1* were performed and normalized to *GAPDH* levels and the $2^{-\Delta CT}$ values from normal and tumor samples were plotted. Horizontal bars show the median value of *ETS1* levels. I, Pearson's *r*-analysis represented as a scatter plot for *SLC7A11* and *ETS1* in the tumor samples. *r* and *P* represent correlation coefficient and *P*-value, respectively. J, Model of the mechanism by which LCN2 promotes therapy resistance and tumor progression

production in the context of chemotherapy. A reduction in intracellular iron levels is observed when LCN2 is over-expressed and is dependent on the ability of LCN2 to bind iron. The ability of LCN2 to bind iron is also required for the ability of LCN2 to inhibit ferroptotic cell death. These results are consistent with the observation that stimulating ferroptosis leads to a reversal of tumor growth and chemo-resistance in multiple tumor types.¹⁰⁻¹⁴ Therefore, the ability to inhibit LCN2 function could be a potential therapeutic strategy for the treatment of multiple tumor types.²⁰

An increase in intracellular iron levels can stimulate Ferroptosis through the activation of iron transport and a reduction of iron import^{53,54} or the autophagy-mediated degradation of ferritin.^{55,56} This report indicates that LCN2 might be required for the export of iron, thereby leading to chemo-resistance, and is consistent with previous reports suggesting that LCN2 might mediate the export of iron under conditions of iron excess.¹⁸ 3D12B2 might prevent the re-import of LCN2 by blocking the association of LCN2 with the LCN2 receptor, thereby resulting in a decrease in intracellular LCN2 levels leading to a reduction in iron export, consistent with our observations that treatment with 3D12B2 results in an increase in the levels of ferrous iron in cells upon treatment with 5FU. Further, treatment with 3D12B2 results in a decrease in the ability to clear peroxidated lipids, which is consistent with the increase in ferrous iron levels, a hallmark of ferroptosis.

In addition to regulating iron levels, our data suggest that LCN2 inhibits ferroptosis by stimulating the expression of the *ETS1* transcription factor, leading to the expression of *GPX4* and *xCT*, which is consistent with previously published data.^{34,57} The induction of *ETS1*, *GPX4* and *xCT* expression is reversed in the LCN2 knockdown clones and upon treatment of LCN2 expressing cell lines with 3D12B2. However, *ETS1* expression might not be sufficient to inhibit ferroptosis in the absence of LCN2 as the ability of LCN2 to bind iron is required to inhibit ferroptosis. While the mechanism underlying the increase in *ETS1* levels upon LCN2 expression is unclear, the stimulation of tyrosine kinase signaling pathways can increase *ETS1* expression.⁵⁸ LCN2 stimulates the re-localization of EGFR to the membrane in models of chronic kidney disease with a concomitant increase in EGFR activity.⁴⁴ Hence, LCN2 might promote *ETS1* expression by inhibiting the degradation of receptor tyrosine kinases in lysosomes, leading to their recycling to the cell surface.⁴⁴ Our observations that loss of either *ETS1* or *xCT* leads to a decrease in cell survival, both in the presence and absence of 5FU, is consistent with the fact that inhibiting LCN2 function in vivo leads to decreased tumor formation in the absence of treatment with 5FU, which is probably due to a decrease in *xCT* levels and an increase in the levels of intracellular iron leading to ferroptosis-mediated cell death.

The results in this report suggest the following model for LCN2-mediated chemo-resistance (Figure 6J). LCN2 inhibits ferroptosis by reducing intracellular iron levels and stimulating the clearance of peroxidated lipids. LCN2 binds iron leading to an inhibition of the conversion of ferric to ferrous iron and promotes iron export. In addition, LCN2 stimulates the expression of *xCT* and *GPX4*, leading to an increase in intracellular glutathione levels and an increased clearance

of peroxidated lipids (Figure 6J). To the best of our knowledge, this is the first example of a gene product that directly impacts both the inhibition of iron accumulation and the reduction of peroxidated lipids. These contribute to the inhibition of ferroptotic cell death and treating these cells with the ferroptosis promoters, erastin and RSL3, or inhibiting LCN2 function by treating cells with a monoclonal antibody to LCN2 leads to increased ferroptotic cell death. We speculate that the antibody inhibits the association of LCN2 with the LCN2 receptor, thereby decreasing intracellular LCN2 levels leading to an increase in intracellular ferrous iron levels and a decrease in the levels of *GPX4* and *xCT*. These results suggest that the inhibition of LCN2 could be an important therapeutic strategy in multiple tumor types and in tumors that are resistant to conventional chemotherapy.

ACKNOWLEDGEMENTS

The authors would like to thank Dr. Sanjeev Galande (IISER Pune) for the DLD1 and HT29 cell lines. The authors would also like to thank Dr. Jayant Goda for help in designing the in vivo radiation experiment, the ACTREC Animal house facility for help with animal experiments and Dr. E.J. Androphy, Dr. S. Rath and Dr. S. Sengupta for critically reading the article, and Dr. C. Travasso for reviewing language use in the article. The work was supported by a grant (BT/PR8351/MED/30/995/2013) from the Department of Biotechnology to SND and the ACTREC donation fund (4338) to SND.

CONFLICT OF INTEREST

The following authors have filed an Indian and PCT patent for the monoclonal antibody 3D12B2 generated in our study: Nazia Chaudhary, Bhagya Shree Choudhary, Sanket Girish Shah, Nileema Khapare, Nehanjal Dwivedi, Rahul Thorat, Smitha P.K., Sujan K. Dhar, Sanjay Gupta, Manjula Das and Sorab N. Dalal. The other authors declare having no conflict of interests associated with this article.

DATA AVAILABILITY STATEMENT

All plasmids generated in this report are available upon signing an MTA from SND or MD. The antibody 3D12B2 can be obtained after signing an MTA from MD and SKD. The data that support the findings of our study are available from the corresponding author upon request.

ORCID

Sorab N. Dalal  <https://orcid.org/0000-0001-6883-7550>

REFERENCES

1. Briffa R, Langdon SP, Grech G, Harrison DJ. Acquired and intrinsic resistance to colorectal cancer treatment. In: Chen J, ed. *Colorectal Cancer - Diagnosis, Screening and Management*. London: Intech Open; 2018:57-81.
2. Vallam KC, Desouza A, Bal M, Patil P, Engineer R, Saklani A. Adenocarcinoma of the rectum-a composite of three different subtypes with varying outcomes? *Clin Colorectal Cancer*. 2016;15:e47-e52.
3. Kozovska Z, Gabrisova V, Kucerova L. Colon cancer: cancer stem cells markers, drug resistance and treatment. *Biomed Pharmacother*. 2014; 68:911-916.

4. Dixon SJ, Stockwell BR. The hallmarks of Ferroptosis. *Ann Rev Cancer Biol.* 2019;3:35-54.
5. Dixon SJ, Lemberg KM, Lamprecht MR, et al. Ferroptosis: an iron-dependent form of nonapoptotic cell death. *Cell.* 2012;149:1060-1072.
6. Yang WS, Kim KJ, Gaschler MM, Patel M, Shchepinov MS, Stockwell BR. Peroxidation of polyunsaturated fatty acids by lipoxygenases drives ferroptosis. *Proc Natl Acad Sci U S A.* 2016;113:E4966-E4975.
7. Yang WS, SriRamaratnam R, Welsch ME, et al. Regulation of ferroptotic cancer cell death by GPX4. *Cell.* 2014;156:317-331.
8. Dixon SJ, Patel DN, Welsch M, et al. Pharmacological inhibition of cystine-glutamate exchange induces endoplasmic reticulum stress and ferroptosis. *Elife.* 2014;3:e02523.
9. Friedmann Angeli JP, Schneider M, Proneth B, et al. Inactivation of the ferroptosis regulator Gpx4 triggers acute renal failure in mice. *Nat Cell Biol.* 2014;16:1180-1191.
10. Dolma S, Lessnick SL, Hahn WC, Stockwell BR. Identification of genotype-selective antitumor agents using synthetic lethal chemical screening in engineered human tumor cells. *Cancer Cell.* 2003;3:285-296.
11. Yagoda N, von Rechenberg M, Zaganjor E, et al. RAS-RAF-MEK-dependent oxidative cell death involving voltage-dependent anion channels. *Nature.* 2007;447:864-868.
12. Yang WS, Stockwell BR. Synthetic lethal screening identifies compounds activating iron-dependent, nonapoptotic cell death in oncogenic-RAS-harboring cancer cells. *Chem Biol.* 2008;15:234-245.
13. Hangauer MJ, Viswanathan VS, Ryan MJ, et al. Drug-tolerant persister cancer cells are vulnerable to GPX4 inhibition. *Nature.* 2017;551:247-250.
14. Viswanathan VS, Ryan MJ, Dhruv HD, et al. Dependency of a therapy-resistant state of cancer cells on a lipid peroxidase pathway. *Nature.* 2017;547:453-457.
15. Chakraborty S, Kaur S, Guha S, Batra SK. The multifaceted roles of neutrophil gelatinase associated lipocalin (NGAL) in inflammation and cancer. *Biochim Biophys Acta.* 1826;2012:129-169.
16. Schmidt-Ott KM, Mori K, Kalandadze A, et al. Neutrophil gelatinase-associated lipocalin-mediated iron traffic in kidney epithelia. *Curr Opin Nephrol Hypertens.* 2006;15:442-449.
17. Playford RJ, Belo A, Poulsom R, et al. Effects of mouse and human lipocalin homologues 24p3/lcn2 and neutrophil gelatinase-associated lipocalin on gastrointestinal mucosal integrity and repair. *Gastroenterology.* 2006;131:809-817.
18. Devireddy LR, Gazin C, Zhu X, Green MR. A cell-surface receptor for lipocalin 24p3 selectively mediates apoptosis and iron uptake. *Cell.* 2005;123:1293-1305.
19. Yan L, Borregaard N, Kjeldsen L, Moses MA. The high molecular weight urinary matrix metalloproteinase (MMP) activity is a complex of gelatinase B/MMP-9 and neutrophil gelatinase-associated lipocalin (NGAL). Modulation of MMP-9 activity by NGAL. *J Biol Chem.* 2001;276:37258-37265.
20. Candido S, Maestro R, Polesel J, et al. Roles of neutrophil gelatinase-associated lipocalin (NGAL) in human cancer. *Oncotarget.* 2014;5:1576-1594.
21. Rodvold JJ, Mahadevan NR, Zanetti M. Lipocalin 2 in cancer: when good immunity goes bad. *Cancer Lett.* 2012;316:132-138.
22. Nielsen BS, Borregaard N, Bundgaard JR, Timshel S, Sehested M, Kjeldsen L. Induction of NGAL synthesis in epithelial cells of human colorectal neoplasia and inflammatory bowel diseases. *Gut.* 1996;38:414-420.
23. Sun Y, Yokoi K, Li H, et al. NGAL expression is elevated in both colorectal adenoma-carcinoma sequence and cancer progression and enhances tumorigenesis in xenograft mouse models. *Clin Cancer Res.* 2011;17:4331-4340.
24. McLean MH, Thomson AJ, Murray GI, Fyfe N, Hold GL, El-Omar EM. Expression of neutrophil gelatinase-associated lipocalin in colorectal neoplastic progression: a marker of malignant potential? *Br J Cancer.* 2013;108:2537-2541.
25. Basu S, Chaudhary N, Shah S, et al. Plakophilin3 loss leads to an increase in lipocalin2 expression, which is required for tumour formation. *Exp Cell Res.* 2018;369:251-265.
26. Kundu ST, Gosavi P, Khapare N, et al. Plakophilin3 downregulation leads to a decrease in cell adhesion and promotes metastasis. *Int J Cancer.* 2008;123:2303-2314.
27. Mir R, Pradhan SJ, Patil P, Mulherkar R, Galande S. Wnt/beta-catenin signaling regulated SATB1 promotes colorectal cancer tumorigenesis and progression. *Oncogene.* 2016;35:1679-1691.
28. Dalal SN, Schweitzer CM, Gan J, DeCaprio JA. Cytoplasmic localization of human cdc25C during interphase requires an intact 14-3-3 binding site. *Mol Cell Biol.* 1999;19:4465-4479.
29. Basu S, Thorat R, Dalal SN. MMP7 is required to mediate cell invasion and tumor formation upon Plakophilin3 loss. *PLoS One.* 2015;10:e0123979.
30. Cerami E, Gao J, Dogrusoz U, et al. The cBio cancer genomics portal: an open platform for exploring multidimensional cancer genomics data. *Cancer Discov.* 2012;2:401-404.
31. Gao J, Aksoy BA, Dogrusoz U, et al. Integrative analysis of complex cancer genomics and clinical profiles using the cBioPortal. *Sci Signal.* 2013;6:l1.
32. Bao G, Clifton M, Hoette TM, et al. Iron traffics in circulation bound to a siderocalin (Ngal)-catechol complex. *Nat Chem Biol.* 2010;6:602-609.
33. Habib E, Linher-Melville K, Lin HX, Singh G. Expression of xCT and activity of system xc(-) are regulated by NRF2 in human breast cancer cells in response to oxidative stress. *Redox Biol.* 2015;5:33-42.
34. Lim JKM, Delaidelli A, Minaker SW, et al. Cystine/glutamate antiporter xCT (SLC7A11) facilitates oncogenic RAS transformation by preserving intracellular redox balance. *Proc Natl Acad Sci U S A.* 2019;116:9433-9442.
35. Ye P, Mimura J, Okada T, et al. Nrf2- and ATF4-dependent upregulation of xCT modulates the sensitivity of T24 bladder carcinoma cells to proteasome inhibition. *Mol Cell Biol.* 2014;34:3421-3434.
36. Santiago-Sanchez GS, Pita-Grisanti V, Quinones-Diaz B, Gumpfer K, Cruz-Monserrate Z, Vivas-Mejia PE. Biological functions and therapeutic potential of Lipocalin 2 in cancer. *Int J Mol Sci.* 2020;21:1-15.
37. Maier HT, Aigner F, Trenkwalder B, et al. Up-regulation of neutrophil gelatinase-associated lipocalin in colorectal cancer predicts poor patient survival. *World J Surg.* 2014;38:2160-2167.
38. Reilly PT, Teo WL, Low MJ, et al. Lipocalin 2 performs contrasting, location-dependent roles in APCmin tumor initiation and progression. *Oncogene.* 2013;32:1233-1239.
39. Kim SL, Lee ST, Min IS, et al. Lipocalin 2 negatively regulates cell proliferation and epithelial to mesenchymal transition through changing metabolic gene expression in colorectal cancer. *Cancer Sci.* 2017;108:2176-2186.
40. Lee HJ, Lee EK, Lee KJ, Hong SW, Yoon Y, Kim JS. Ectopic expression of neutrophil gelatinase-associated lipocalin suppresses the invasion and liver metastasis of colon cancer cells. *Int J Cancer.* 2006;118:2490-2497.
41. De Bundel D, Schallier A, Loyens E, et al. Loss of system x(c)- does not induce oxidative stress but decreases extracellular glutamate in hippocampus and influences spatial working memory and limbic seizure susceptibility. *J Neurosci.* 2011;31:5792-5803.
42. Flo TH, Smith KD, Sato S, et al. Lipocalin 2 mediates an innate immune response to bacterial infection by sequestering iron. *Nature.* 2004;432:917-921.
43. Ghosh S, Padmanabhan A, Vaidya T, et al. Neutrophils homing into the retina trigger pathology in early age-related macular degeneration. *Commun Biol.* 2019;2:348.

44. Yamine L, Zablocki A, Baron W, Terzi F, Gallazzini M. Lipocalin-2 regulates epidermal growth factor receptor intracellular trafficking. *Cell Rep*. 2019;29:2067-2077. e6.
45. Brookes MJ, Hughes S, Turner FE, et al. Modulation of iron transport proteins in human colorectal carcinogenesis. *Gut*. 2006;55:1449-1460.
46. Torti SV, Torti FM. Iron and cancer: more ore to be mined. *Nat Rev Cancer*. 2013;13:342-355.
47. Torti SV, Torti FM. Iron: the cancer connection. *Mol Aspects med*. 2020;100860.
48. Nelson RL. Iron and colorectal cancer risk: human studies. *Nutr Rev*. 2001;59:140-148.
49. Radulescu S, Brookes MJ, Salgueiro P, et al. Luminal iron levels govern intestinal tumorigenesis after Apc loss in vivo. *Cell Rep*. 2012;2:270-282.
50. Toyokuni S. Iron-induced carcinogenesis: the role of redox regulation. *Free Radic Biol Med*. 1996;20:553-566.
51. Myant KB, Cammareri P, McGhee EJ, et al. ROS production and NF-kappaB activation triggered by RAC1 facilitate WNT-driven intestinal stem cell proliferation and colorectal cancer initiation. *Cell Stem Cell*. 2013;12:761-773.
52. Wang C, Li P, Xuan J, et al. Cholesterol enhances colorectal cancer progression via ROS elevation and MAPK signaling pathway activation. *Cell Physiol Biochem*. 2017;42:729-742.
53. Gao M, Monian P, Quadri N, Ramasamy R, Jiang X. Glutaminolysis and transferrin regulate ferroptosis. *Mol Cell*. 2015;59:298-308.
54. Ma S, Henson ES, Chen Y, Gibson SB. Ferroptosis is induced following siramesine and lapatinib treatment of breast cancer cells. *Cell Death Dis*. 2016;7:e2307.
55. Gao M, Monian P, Pan Q, Zhang W, Xiang J, Jiang X. Ferroptosis is an autophagic cell death process. *Cell Res*. 2016;26:1021-1032.
56. Hou W, Xie Y, Song X, et al. Autophagy promotes ferroptosis by degradation of ferritin. *Autophagy*. 2016;12:1425-1428.
57. Verschoor ML, Singh G. Ets-1 regulates intracellular glutathione levels: key target for resistant ovarian cancer. *Mol Cancer*. 2013;12:138.
58. Dittmer J. The biology of the Ets1 proto-oncogene. *Mol Cancer*. 2003;2:29.

SUPPORTING INFORMATION

Additional supporting information may be found online in the Supporting Information section at the end of this article.

How to cite this article: Chaudhary N, Choudhary BS, Shah SG, et al. Lipocalin 2 expression promotes tumor progression and therapy resistance by inhibiting ferroptosis in colorectal cancer. *Int. J. Cancer*. 2021;149(7):1495–1511. <https://doi.org/10.1002/ijc.33711>